

Intra- and Intermolecular Inhomogeneities in the Course of Glassy Densification of Polyalcohols

Jan Philipp Gabriel,^{*} Martin Tress^{*,†} Wilhelm Kossack, Ludwig Popp,[‡] and Friedrich Kremer[§]
Peter Debye Institute for Soft Matter Research, Leipzig University, 04103 Leipzig, Germany
 (Dated: September 8, 2020)

To test basic assumptions inherent to most theories of molecular liquids and glasses, Infrared spectroscopy is carried out on short polyalcohols at temperatures ranging from far above to far below their glass transition. By analyzing specific vibrations, the thermal expansion of covalent bonds and hydrogen bridges is determined revealing striking differences. A comparison with density verifies the negligibility of *intramolecular* expansion but exposes severe inhomogeneities on *intermolecular* scale. This signals distinct roles in glassy densification and promotes an atomistic understanding.

The vitrification of a (super-cooled) liquid into a disordered solid is a central subject of experimental and theoretical soft condensed matter research [1–12]. A distinctive feature of super-cooled liquids and glasses is their diverging molecular fluctuation rate. Even simple concepts like the free volume model [13–16] relate this to the reduction of intermolecular volume, in other words an increase in density, reflected in the term glassy densification. While the free volume model uses the inhomogeneity of the density only conceptually, early microscopic theories of liquids identify it as an additional key quantity [17]. This has also been established for glasses [18–20], and it became clear that heterogeneity in time and space, in other words a varying temporal and spatial scale on which molecules fluctuate [21, 22] is a fundamental attribute of both liquids and glasses. Consequently, modern theoretical approaches like the random first order transition (RFOT) theory [9, 23, 24] incorporate an inhomogeneous density in their description.

Interestingly, even RFOT theory, one of the most sophisticated concepts of molecular glasses, is based on abstract beads and their packing density [9], i.e. particular intermolecular interactions are not specifically considered. Hence, this approach assumes that the impact of intermolecular interactions on structural relaxation is described by (packing) density. This means that certain presumptions are inherent to this model (similar to most other theoretical descriptions [9, 25–29]): i) *intramolecular* expansion is neglected [30], i.e. density changes are fully or almost fully ascribed to *intermolecular* expansion, and ii) no directionality or inhomogeneity of the *intermolecular* interactions is accounted for, i.e. the thermal expansion even on molecular scale is considered isotropic. While the first conjecture appears rather plausible, the second one is questionable for a vast range of systems involving directional interactions e.g. hydrogen (H-) bridges as in glycerol, one of the most studied model glass formers [31–39]. Despite their essential nature, to the best of our knowledge these two conjectures, negligibility of *intramolecular* expansion and *intermolecular* bond directionality, have not yet been tested experimentally.

Here, we reexamine our previously published Infrared (IR) spectroscopy data of short polyalcohols from a wide temperature range above and below the calorimetric glass transition temperature T_g [40]. These molecules (glycerol, threitol, xylitol, and sorbitol) have a regular structure but the orientation of the hydroxy groups, which associate and form a H-bridge network, gives rise to a significant anisotropy. This *intramolecular* inhomogeneity leads to weak and strong *intermolecular* H-bridges, and with a novel extensive analysis we reveal their individual thermal expansions. Despite the supramolecular network formed by the mildly expanding strong H-bridges, the profoundly expanding weak H-bridges surprisingly allow for considerable changes in density. A consequence of this inhomogeneity of the *intermolecular* interactions is a decoupling of the structural relaxation (governed by strong bridges) from the thermal expansivity and density (dominated by weak bridges).

IR spectra were recorded using a Fourier transform infrared (FTIR) spectrometer (Bio–Rad FTS 6000) combined with an IR microscope (UMA 500) and a liquid nitrogen-cooled mercury-cadmiumtelluride (MCT) detector (Kolmar Technologies, Inc, USA) while a THMS 350V stage (Linkam Scientific Instruments, UK) flushed with dry nitrogen controlled the sample temperature; further information can be found elsewhere [40]. Comparing the spectra of the polyalcohols under study reveals their molecular characteristics (Fig. 1a). In the low frequency range ($\bar{\nu} = 800 - 1200 \text{ cm}^{-1}$) the CO stretching vibration $\nu(\text{CO})$ at $\bar{\nu} \approx 1125 \text{ cm}^{-1}$ and a combined CCO stretching vibration $\nu(\text{CCO})$ at $\bar{\nu} \approx 860 - 890 \text{ cm}^{-1}$ exhibit bands distinctive for each substance (Fig. 1b). The $\nu(\text{CO})$ vibration shows only minor changes, i.e. a shift to higher frequencies with increasing molecular weight by $\sim 20 \text{ cm}^{-1}$ from glycerol to sorbitol. In contrast, the $\nu(\text{CCO})$ band not only shifts by $\sim 40 \text{ cm}^{-1}$ but also undergoes pronounced changes in shape for each material due to superimposing complex structural oscillations. Density functional theory (DFT) calculations of glycerol reveal distinct spectra for the various conformers in this frequency range [41]. Since a change in molecular weight alters not only the number of conformers but also

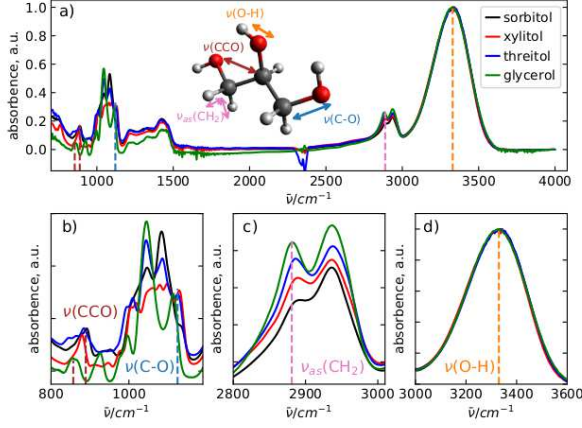


FIG. 1. a) IR absorbance spectra of several polyalcohols as indicated at selected temperatures (sorbitol: 249.4 K, xylitol: 252.5 K, threitol: 269.2 K, and glycerol: 269.2 K) to show identical spectral positions of the $\nu(\text{OH})$ band (dashed orange line); the absorbance is normalized to the $\nu(\text{OH})$ peak. Close-ups of the spectral regions of b) the $\nu(\text{CCO})$ band (brown dashed line) and the $\nu(\text{CO})$ band (blue dashed line), c) the $\nu_{as}(\text{CH}_2)$ band (pink dashed line), and d) the $\nu(\text{OH})$ band (orange dashed line). The colored arrows in the molecular model of glycerol in a) exemplify the respective vibrations. The experimental uncertainty is smaller than the line width.

their probability distribution, such spectral differences are expected, and, due to their complexity, the absorption bands cannot be unraveled any further.

At higher frequencies, the vibrations become more localized and hence less complex, but also less distinct in the homologous series. Thus, the spectral region indicative of CH stretching vibrations ($\bar{\nu} = 2800 - 3000 \text{ cm}^{-1}$) exhibits only minor differences (Fig. 1c). The asymmetric CH_2 stretching vibration $\nu_{as}(\text{CH}_2)$ at $\bar{\nu} \approx 2880 \text{ cm}^{-1}$ shifts by less than 5 cm^{-1} from glycerol to sorbitol; its absorbance reduces with increasing molecular weight since CH_2 stretching happens only at terminal carbons. Conversely, the absorbance of CH stretching $\nu(\text{CH})$ (from non-terminal carbons) at $\bar{\nu} \approx 2950 \text{ cm}^{-1}$ increases; however, since it is superimposed by the symmetric CH_2 stretching vibration $\nu_{sm}(\text{CH}_2)$ at $\bar{\nu} \approx 2940 \text{ cm}^{-1}$ and the tail of the OH stretching vibration band $\nu(\text{OH})$, only $\nu_{as}(\text{CH}_2)$ is analyzed quantitatively. At even higher frequencies ($\bar{\nu} = 3000 - 3600 \text{ cm}^{-1}$), the broad $\nu(\text{OH})$ peak, typical for alcohols [42], at $\bar{\nu} \approx 3350 \text{ cm}^{-1}$ is prominent and identical in shape in all four polyalcohols (Fig. 1d).

From the spectra, peak frequencies of the $\nu(\text{OH})$, $\nu_{as}(\text{CH}_2)$, and $\nu(\text{CO})$ band were determined in a wide temperature range (Fig. 2). The $\nu(\text{OH})$ band exhibits a large red-shift with decreasing temperature (Fig. 2a) amounting to $\sim 60 \text{ cm}^{-1}/100 \text{ K}$ above T_g in all substances. Further, the temperature dependence of the peak frequency has a distinct change of slope at T_g (similar to density). In contrast, the red-shift upon tempera-

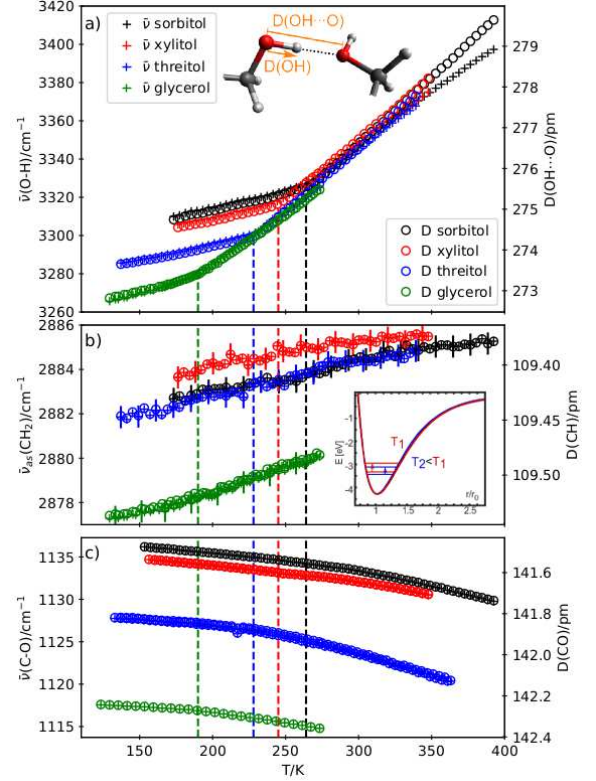


FIG. 2. Temperature dependence of the IR absorption frequencies of the a) $\nu(\text{OH})$, b) $\nu_{as}(\text{CH}_2)$, and c) $\nu(\text{CO})$ bands (crosses, left axis) for different polyalcohols as indicated. The conversion of stretching frequencies into lengths (circles, right axis) of hydrogen bridges and covalent bonds is done via eq. (3) for $\nu(\text{OH})$, and via a calibrated eq. (2) for $\nu(\text{CH})$ and $\nu(\text{CO})$ (see text), respectively. Dashed vertical lines indicate each material's T_g (same color code). The inset sketches vibrational states in the Morse potential at two different temperatures. The experimental uncertainty is smaller than the symbol size unless indicated otherwise.

ture reduction observed in the $\nu_{as}(\text{CH}_2)$ band is as small as 3 cm^{-1} in the entire range ($150 - 250 \text{ K}$), and shows no distinct feature at T_g (Fig. 2b). The $\nu(\text{CO})$ bands exhibit a small ($\sim 5 \text{ cm}^{-1}$ in the whole range) blue-shift as temperature decreases (Fig. 2c) with a gradually changing slope above T_g (though not as distinct as in $\nu(\text{OH})$).

A shift in IR absorption frequency of a stretching vibration typically reflects a change in bond length [43, 44]. Consequently, the large shift in $\nu(\text{OH})$ means that the overall *intramolecular* thermal expansion is dominated by changes in OH length while variations in CH and CO lengths have only minor impact. Since a red-shift indicates an expansion (weakening of the bond), both OH and CH bond lengths increase upon cooling (Fig. 2a & b). This is caused by the respective *intermolecular* interactions, i.e. strong $(\text{OH} \cdots \text{O})$ and weak $(\text{CH} \cdots \text{O})$ H-bridges. A densification with decreasing temperature reduces *intermolecular* distances and brings the oxy-

gen atoms of surrounding molecules (H-bridge acceptors) closer. Hence, the (*intermolecular*) H-bridges become stronger while the (*intramolecular*) covalent bonds are stretched [45]. In contrast, the blue-shift upon cooling in $\nu(\text{CO})$ (Fig. 2c) implies a contraction of the covalent bonds in the backbone (i.e. normal thermal expansion).

In a simple quantitative approach, the change in bond length is approximated by employing the Morse potential [46–48] to describe molecular vibrations (Fig. 2 inset):

$$V(r) = E_d(1 - \exp[-a(r - r_0)])^2 \quad (1)$$

Here, E_d represents the dissociation energy and a the inverse width of the potential. The latter can be related analytically to the difference of the energy eigenvalues in the ground state and the first excited state $\Delta E(\bar{\nu})$:

$$a(E(\bar{\nu}), E_d) = \sqrt{\frac{\mu}{2\hbar^2}} \left(\sqrt{E_d} - \sqrt{E_d - 2\Delta E(\bar{\nu})} \right) \quad (2)$$

Therein, μ is the reduced mass and \hbar the reduced Planck constant. Using typical dissociation energies (e.g. from dimethylether $E_d(\text{CO}) = 325 \text{ kJ/mol}$ [49] and methane $E_d(\text{CH}) = 435 \text{ kJ/mol}$ [50]) and inserting the measured IR absorption frequencies $\bar{\nu}(T)$ via $\Delta E(\bar{\nu}(T)) = 2\pi\hbar\bar{\nu}(T)$ yields $1/a(T)$, an estimate for the change in interatomic (i.e. *intramolecular*) distance with temperature. In order to approximate the absolute length of a bond $D(T)$ (Fig. 2b & c), the respective interatomic distance obtained from DFT calculations [51] of glycerol D^{gly} were used for a calibration $D^{gly} = D(T_{ref}) = 1/a(T_{ref}) + D_0$ at the reference temperature $T_{ref} = 300 \text{ K}$ with the correction D_0 ($D_{CH} = 109.47 \text{ pm}$, and $D_{CO}^{gly} = 142.4 \text{ pm}$ with $D_{0,CH} = 54.8 \text{ pm}$, and $D_{0,CO}^{gly} = 96.4 \text{ pm}$ respectively). Extended DFT calculations to reproduce a temperature dependence fail since *intermolecular* interactions are missing. (The latter are required to model an equilibrated, i.e. energetically minimized bond at different lengths). Therefore, eq. (2) is used to quantify the bond lengths D_{CH} and D_{CO} [52].

For the OH bond as well as the respective $\text{OH}\cdots\text{O}$ bridge however, there exists a vast record of experimental work on lengths, among them also correlations to IR absorption frequencies. Studies of crystalline H-bonding materials combined X-ray and neutron diffraction with IR spectroscopy to deduce the relation between the *intermolecular* $\text{OH}\cdots\text{O}$ distance $D_{\text{OH}\cdots\text{O}}$ and the peak position $\bar{\nu}(\text{OH})$ (i.e. the respective *intramolecular* OH vibration) [53, 54]. The found empirical relation [53] to extract $D(\text{OH}\cdots\text{O})$ (Fig. 2a) is given by:

$$D_{\text{OH}\cdots\text{O}}(\bar{\nu}) = 13.21 \log \left(\frac{304 \cdot 10^9}{3592 - \bar{\nu} \cdot \text{cm}} \right) \text{ pm} \quad (3)$$

Furthermore, these structural investigations established a relation between $D_{\text{OH}\cdots\text{O}}$ and D_{OH} [54] which is used to obtain also the temperature dependence of the latter.

The thermal expansion of both $D_{\text{OH}\cdots\text{O}}$ and D_{OH} exhibits a characteristic kink at T_g (Fig. 3a & b), like the underlying peak frequency of $\nu(\text{OH})$. Changes in density (indicating T_g) originate from *inter*- and *intramolecular* expansion; however, their respective contribution is yet unknown. For quantitative evaluation, we use the cubic root of the specific volume obtained from the mass density of glycerol $\rho(T)$ [55] and its molar mass M as reference. The resulting length $D_{mol} = \sqrt[3]{M/(\rho N_A)}$ (where N_A is Avogadro's number) resembles the average distance between the centers of adjacent molecules (i.e. a 1-dimensional equivalent to specific volume).

While vibrational spectroscopy provides no direct access to bond lengths (i.e. structural methods are required to establish a correlation), its extremely high resolution is excellent to trace changes [56]. Consequently, in the following we focus on these (absolute) changes using the respective value at T_g as reference ($\Delta D(T) = D(T) - D(T_g)$). A comparison of ΔD_{mol} with ΔD_{OH} , ΔD_{CH} , and ΔD_{CO} reveals that all these *intramolecular* lengths exhibit a much weaker thermal expansion (about a factor of 20 for ΔD_{OH} and more than a factor of 100 for ΔD_{CH} and ΔD_{CO}), and thus are negligible in the densification of the material (Fig. 3a). Consequently, the expansion of *intermolecular* bridges must dominate densification. However, the change in $\Delta D_{\text{OH}\cdots\text{O}}$ is by about a factor of 3 smaller than in ΔD_{mol} . Considering the chemical structure of glycerol, the only other *intermolecular* interactions are of van der Waals type and weak $\text{CH}\cdots\text{O}$ H-bridges [52]. The red-shift of $\nu_{as}(\text{CH}_2)$ with decreasing temperature indicates the latter. It is known that this type of bridge has a length of $\sim 350 \text{ pm}$ [52], considerably longer than $D_{\text{OH}\cdots\text{O}}$ ($\sim 280 \text{ pm}$). Attempts to establish a relation between $\nu_{as}(\text{CH}_2)$ and $D_{\text{CH}\cdots\text{O}}$, based on studies of crystalline materials [52, 57], in order to extract a reliable temperature dependence fail because of too much scattering of the data. Additionally, due to the low polarity of the CH bond, its length is rather insensitive to the presence of H-bridge acceptors (in weak H-bridges longer than 300 pm , the distance between hydrogen and the H-bridge acceptor varies strongly, i.e. several tens of pm , while the change in donor bond length is $< 1 \text{ pm}$ [58], for $-\text{CH}\cdots\text{O}$ even $< 0.1 \text{ pm}$ [57, 59]).

The overall thermal expansion $\Delta D_{mol}(T)$ is an average of all *intra*- and *intermolecular* expansivities. Since the former are negligible compared to the latter, we approximate $\Delta D_{mol}(T)$ as composition of *intermolecular* expansions only:

$$\Delta D_{mol}(T) = \phi_{\text{OH}} \Delta D_{\text{OH}\cdots\text{O}}(T) + \phi_{\text{CH}} \Delta D_{\text{CH}\cdots\text{O}}(T) \quad (4)$$

Here, ϕ_{OH} and ϕ_{CH} are weighing factors representing the fraction of OH and CH donors per molecule, respectively (e.g. for glycerol $\phi_{\text{OH}} = 3/8$ and $\phi_{\text{CH}} = 5/8$). Insertion of ΔD_{mol} obtained from density and $\Delta D_{\text{OH}\cdots\text{O}}$ calculated from eq. (3) yields an approximation for the ther-

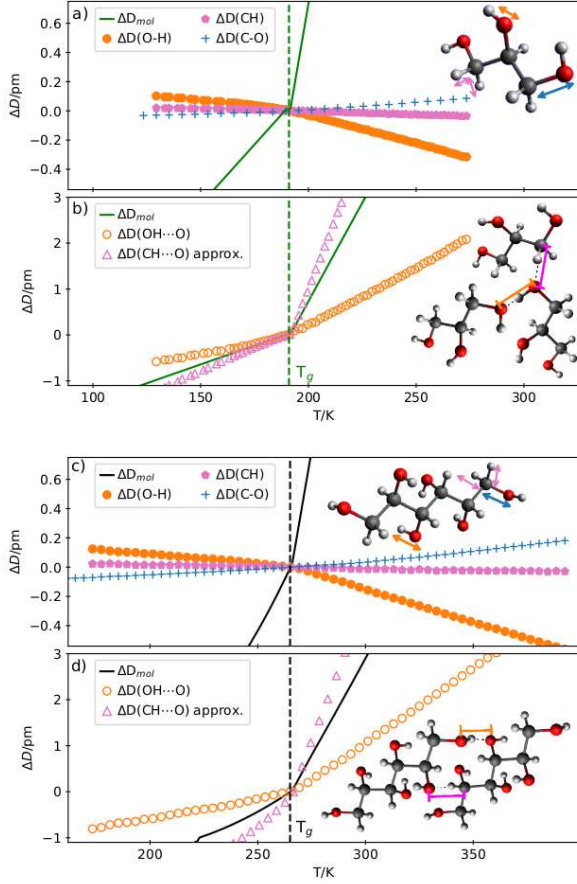


FIG. 3. Absolute expansion of a) *intra*- and b) *inter*molecular distances, bond and hydrogen bridge lengths in glycerol, and c) and d) in sorbitol, respectively. ΔD_{mol} is calculated from the mass densities [60] taken from [55, 61]. T_g is indicated by a dashed vertical line. The arrows in the sketched molecules indicate the respective stretching vibrations of the bonds and lengths of the hydrogen bridges (same color code as the symbols). The uncertainty originating from the experimental error of the IR measurements is smaller than the symbol size.

mal expansion $\Delta D_{CH\cdots O}(T)$ (Fig. 3b) which is by about a factor of 6 larger than $\Delta D_{OH\cdots O}(T)$. Despite the lack of direct experimental data it is conceivable: due to their increased length and low polarity the $CH\cdots O$ bridges are more susceptible to temperature change than the $OH\cdots H$ bridges. Also, studies of semi-crystalline poly(3-hydroxybutyrate) reported thermally induced changes of inter-chain distance in the crystallites, which is governed by $CH\cdots O$ contacts (of methyl groups and ketones, i.e. different chemical structure), of $\sim 10\text{ pm}$ accompanied by shifts in $\nu(\text{CH}_2)$ of $\sim 3\text{ cm}^{-1}$ [62] (the expansion of $\Delta D_{CH\cdots O}$ estimated from eq. (4) is $\sim 3\text{ pm/cm}^{-1}$).

In sorbitol, the thermal expansion of the different *intra*- and *inter*molecular lengths is almost identical to those in glycerol (Fig. 3). The only deviation is a slightly larger rate of $\Delta D_{OH\cdots O}$ in sorbitol, probably due to the

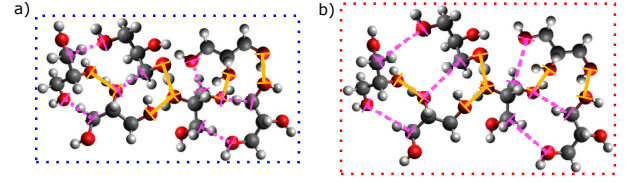


FIG. 4. Sketch of glycerol molecules to exemplify the transition from a) higher to b) lower density (dotted boxes visualize the specific volume of the same six molecules) at minimal expansion of strong $\text{OH}\cdots\text{O}$ H-bridges (orange solid lines). This is realized by expansion of weak $\text{CH}\cdots\text{O}$ H-bridges (magenta dashed lines) and possibly conformational changes.

elevated temperature. This striking similarity indicates that, despite increased molecular weight and number of conformations, density is controlled by the same mechanism. Although we have no extended density data for xylitol and threitol available, the similarity of their IR band evolution suggest an analogous picture. Hence, the view [63] is corroborated that glassy densification in these polyalcohols follows the same physical mechanisms [64–66].

Despite the fact that the biggest thermal expansion of these polyalcohols is found in the $\text{CH}\cdots\text{O}$ bridges, $\bar{\nu}_{CH}(T)$ does not exhibit a characteristic feature at T_g - in contrast to the pronounced kink at T_g in $\bar{\nu}_{OH}(T)$. Consequently, the picture is nurtured that the $\text{OH}\cdots\text{O}$ bridges govern dynamics since these pose the largest energetic barriers to structural relaxation while their impact on overall thermal expansion is small (evidenced by the reduced temperature dependence of density with increasing number of H-bridging groups [67]). That is because (weak) $\text{CH}\cdots\text{O}$ bridges enable considerable changes in average *inter*molecular distance and thus density (Fig. 4) while the network topology is stabilized by mildly expanding (strong) $\text{OH}\cdots\text{O}$ bridges.

That may illuminate a yet unresolved observation reported in the frame of the density scaling concept [68, 69]. In this empirical approach, the structural relaxation time is considered to scale with the term ρ^γ/T with the exponent γ [68, 70]. While many van der Waals liquids obey this scaling [65, 71], particularly associating liquids (and some polymers) defy it [65, 68, 71, 72]. This defiance is caused by the difference in thermal expansion of strong and weak *inter*molecular bridges; their selective impact on density and structural relaxation loosens the relation between the latter two properties which in turn disrupts the scaling. From the interpretation that γ is connected to the (uni-form) *inter*molecular potential [68, 73], one can infer that the reason is the negligence of different (or inhomogeneous) *inter*molecular interactions. This corroborates previous views, that glycerol in particular and possibly associating liquids in general do not comply with common theories of glassy densification [74]. Reports of separated rotational and translational

dynamics in glycerol attributed to the H-bridge network fortify this [75, 76]. Since density scaling also fails in some polymers [77], our results likely reach beyond associating liquids.

In summary, the presented study evidences inhomogeneities of the thermal expansion on both *intra*- (Fig. 3a & c) and *intermolecular* (Fig. 3b & d) scale in the course of glassy densification. In turn, two fundamental presumptions which are inherent to most theoretical models of molecular liquids and their glass transition are checked experimentally (for short polyalcohols): firstly, it is confirmed that *intramolecular* expansion is negligibly small compared to *intermolecular* expansion. Secondly, the assumption of isotropic *intermolecular* interactions is an oversimplification in these systems. In contrast to the extreme cases of glass formation where the inhomogeneity of thermal expansion is negligible, i.e. inorganic glasses (like silica) characterized by extremely strong covalent bonds on the one hand and van der Waals glasses dominated by rather uniform weak interactions on the other hand, many molecular glasses contain both strong and weak interactions simultaneously. Particularly, the different impact of strong and weak bridges on structural relaxation and on density loosens the relation between the latter two properties which likely causes the open questions in the description of associating liquids [69]. All this should motivate the consideration of distinct atomistic interactions in order to gain a molecular understanding of the dynamic glass transition in organic matter. To what extent these findings apply beyond associating liquids to complex glass forming systems in general, remains a challenge for future experimental and theoretical work.

ACKNOWLEDGEMENT

Financial support by the German Science Foundation (DFG) within the collaborative research center SFB TRR 102, sub-projects B08 and B15, respectively, is highly appreciated.

* These authors contributed equally.

† Correspondence to: martin.tress@uni-leipzig.de

‡ Present address: TUD

§ Correspondence to: fkremer@physik.uni-leipzig.de

- [1] Wong, J.; Angell, C. *Glass: Structure by Dynamics*; Marcel Dekker, New York, 1976.
- [2] Anderson, P. W. In *Ill-Condensed Matter*; Balian, R., Maynard, R., Toulouse, G., Eds.; North-Holland, Amsterdam, 1979; pp 159–261.
- [3] Donth, E. J. *Glasübergang*; Akademie-Verlag, Berlin, 1981.
- [4] Zallen, R. *The Physics of Amorphous Solids*; John Wiley & Sons, Ltd, 1983.
- [5] Elliott, S. *Physics of amorphous materials*; Harlow, Essex, England: Longman Scientific & Technical; New York: J. Wiley, 1990.
- [6] Donth, E. J. *Relaxation and thermodynamics in polymers glass transition*; Akademie Verlag GmbH, Berlin, 1992.
- [7] Donth, E. J. *The Glass Transition*; Springer-Verlag Berlin Heidelberg, 2001.
- [8] Kremer, F.; Schönhals, A. *Broadband Dielectric Spectroscopy*, 1st ed.; Springer, 2002.
- [9] Lubchenko, V.; Wolynes, P. G. Theory of Structural Glasses and Supercooled Liquids. *Annual Review of Physical Chemistry* **2007**, *58*, 235–266.
- [10] Ngai, K. *Relaxation and Diffusion in Complex Systems*; Springer-Verlag New York, 2011.
- [11] Götze, W. *Complex Dynamics of Glass-Forming Liquids: A Mode-Coupling Theory*; Oxford University Press, 2012.
- [12] Kremer, F.; Loidl, A. *The Scaling of Relaxation Processes*; Advances in Dielectrics; Springer International Publishing, 2018.
- [13] Fox, T.; Flory, P. Second-Order Transition Temperatures and Related Properties of Polystyrene. I. Influence of Molecular Weight. *Journal of Applied Physics* **1950**, *21*, 581 – 591.
- [14] Fox, T.; Flory, P. Further Studies on the Melt Viscosity of Polyisobutylene. *Journal of Physical Chemistry* **1951**, *55*, 221 – 234.
- [15] Fox, T.; Flory, P. The glass temperature and related properties of polystyrene. Influence of molecular weight. *Journal of Polymer Science* **1954**, *14*, 315 – 319.
- [16] Turnbull, D.; Cohen, M. Free-Volume Model of the Amorphous Phase: Glass Transition. *Journal of Chemical Physics* **1961**, *34*, 120 – 125.
- [17] Bernal, J. An attempt at a molecular theory of liquid structure. *Transactions of the Faraday Society* **1937**, *33*, 27 – 40.
- [18] Ediger, M. Can density or entropy fluctuations explain enhanced translational diffusion in glass-forming liquids? *Journal of Non-Crystalline Solids* **1998**, *235-237*, 10 – 18.
- [19] Donth, E. Dynamic or configurational approach to the glass transition? *Journal of Non-Crystalline Solids* **2002**, *307-310*, 364 – 375.
- [20] Rissanou, A. N.; Harmandaris, V. Structural and Dynamical Properties of Polystyrene Thin Films Supported by Multiple Graphene Layers. *Macromolecules* **2015**, *48*, 2761–2772.
- [21] Ediger, M. Spatially Heterogeneous Dynamics in Supercooled Liquids. *Ann. Rev. Phys. Chem.* **2000**, *51*, 99.
- [22] Richert, R. Heterogeneous dynamics in liquids: fluctuations in space and time. *J. Phys.: Condens. Matter* **2002**, *14*, R703–R738.
- [23] Xia, X.; Wolynes, P. G. Fragilities of liquids predicted from the random first order transition theory of glasses. *Proceedings of the National Academy of Sciences* **2000**, *97*, 2990–2994.
- [24] Stevenson, J. D.; Wolynes, P. G. Thermodynamic-Kinetic Correlations in Supercooled Liquids: A Critical Survey of Experimental Data and Predictions of the Random First-Order Transition Theory of Glasses. *The Journal of Physical Chemistry B* **2005**, *109*, 15093–15097.
- [25] Dyre, J. C. Colloquium: The glass transition and elastic models of glass-forming liquids. *Rev. Mod. Phys.* **2006**, *78*, 953–972.

- [26] Mirigian, S.; Schweizer, K. S. Elastically cooperative activated barrier hopping theory of relaxation in viscous fluids. II. Thermal liquids. *The Journal of Chemical Physics* **2014**, *140*, 194507.
- [27] Mauro, J. C.; Allan, D. C.; Potuzak, M. Nonequilibrium viscosity of glass. *Phys. Rev. B* **2009**, *80*, 094204.
- [28] Bosse, J.; Götze, W.; Lücke, M. Mode-coupling theory of simple classical liquids. *Phys. Rev. A* **1978**, *17*, 434–446.
- [29] Adam, G.; Gibbs, J. H. On the Temperature Dependence of Cooperative Relaxation Properties in Glass-Forming Liquids. *The Journal of Chemical Physics* **1965**, *43*, 139–146.
- [30] If several beads describe one molecule, some *intramolecular* expansion may be formally included but is not distinguished from *intermolecular* expansion.
- [31] Schneider, U.; Lunkenheimer, P.; Brand, R.; Loidl, A. Dielectric and far-infrared spectroscopy of glycerol. *Journal of Non-Crystalline Solids* **1998**, *235–237*, 173 – 179.
- [32] Wuttke, J.; Hernandez, J.; Li, G.; Coddens, G.; Cummins, H. Z.; Fujara, F.; Petry, W.; Sillescu, H. Neutron and light scattering study of supercooled glycerol. *Phys. Rev. Lett.* **1994**, *72*, 3052–3055.
- [33] Klieber, C.; Hecksher, T.; Pezeril, T.; Torchinsky, D. H.; Dyre, J. C.; Nelson, K. A. Mechanical spectra of glass-forming liquids. II. Gigahertz-frequency longitudinal and shear acoustic dynamics in glycerol and DC704 studied by time-domain Brillouin scattering. *J. Chem. Phys.* **2013**, *138*, 12A544.
- [34] Jensen, M. H.; Gainaru, C.; Alba-Simionesco, C.; Hecksher, T.; Niss, K. Slow rheological mode in glycerol and glycerol–water mixtures. *Phys. Chem. Chem. Phys.* **2018**, *20*, 1716–1723.
- [35] Capponi, S.; Napolitano, S.; Behrnd, N. R.; Couderc, G.; Hulliger, J.; Wübbenhorst, M. Structural Relaxation in Nanometer Thin Layers of Glycerol. *The Journal of Physical Chemistry C* **2010**, *114*, 16696–16699.
- [36] Ryabov, Y. E.; Hayashi, Y.; Gutina, A.; Feldman, Y. Features of supercooled glycerol dynamics. *Phys. Rev. B* **2003**, *67*, 132202.
- [37] Beevers, M. S.; Elliott, D. A.; Williams, G. Static and dynamic Kerr-effect studies of glycerol in its highly viscous state. *J. Chem. Soc., Faraday Trans. 2* **1980**, *76*, 112–121.
- [38] Mehl, P. M. Determination of enthalpy relaxation times using traditional differential scanning calorimetry for glycerol and for propylene glycol. *Thermochimica Acta* **1996**, *272*, 201 – 209, Advances in International Thermal Sciences: Environment, Polymers, Energy and Techniques.
- [39] Gabriel, J. P.; Zourchang, P.; Pabst, F.; Helblingand, A.; Weigand, P.; Böhmerand, T.; Blochowicz, T. Intermolecular Cross-Correlations in the Dielectric Response of Glycerol. *arXiv preprint arXiv:1911.10976* **2019**,
- [40] Kremer, F.; Kossack, W.; Anton, A. M. In *The Scaling of Relaxation Processes*; Kremer, F., Loidl, A., Eds.; Springer International Publishing, 2018; pp 61–76.
- [41] Chelli, R.; Gervasio, F. L.; Gellini, C.; Procacci, P.; Cardini, G.; Schettino, V. Density Functional Calculation of Structural and Vibrational Properties of Glycerol. *J. Phys. Chem. A* **2000**, *104*, 5351–5357.
- [42] Bauer, S.; Stern, J.; Böhm, F.; Gainaru, C.; Havenith, M.; Loerting, T.; Böhmer, R. Vibrational study of anharmonicity, supramolecular structure, and hydrogen bonding in two octanol isomers. *Vibrational Spectroscopy* **2015**, *79*, 59 – 66.
- [43] Generally, a shift in band position of a stretching vibration can have different causes; however, gradual shifts on heating/cooling reflect changes in respective bond length.
- [44] Schrader, B. In *Infrared and Raman Spectroscopy*; Schrader, B., Ed.; VCH, Weinheim, 1995; pp 7–62.
- [45] We note that the following neutron scattering study, which employed fits of atom correlation models, claims that glycerol does not form CH \cdots O bridges; however, this conclusion is indirect and incompatible to the red-shift observed in the $\nu_{as}(\text{CH}_2)$ band. Towey, J. J.; Soper, A. K.; Dougan, L. The structure of glycerol in the liquid state: a neutron diffraction study. *Phys. Chem. Chem. Phys.* **2011**, *13*, 9397–9406.
- [46] Morse, P. M. Diatomic Molecules According to the Wave Mechanics. II. Vibrational Levels. *Phys. Rev.* **1929**, *34*, 57–64.
- [47] Dahl, J. P.; Springborg, M. The Morse oscillator in position space, momentum space, and phase space. *The Journal of Chemical Physics* **1988**, *88*, 4535–4547.
- [48] de Lima, E. F.; Hornos, J. E. M. Matrix elements for the Morse potential under an external field. *Journal of Physics B Atomic Molecular Physics* **2005**, *38*, 815–825.
- [49] Pacey, P. D. The Initial Stages of the Pyrolysis of Dimethyl Ether. *Canadian Journal of Chemistry* **1975**, *53*, 2742–2747.
- [50] Benson, S. W.; O’Neal, H. E. *Kinetic data on gas phase unimolecular reactions*; NSRDS-NBS21, 1970.
- [51] Neese, F. Software update: the ORCA program system, version 4.0. *Wiley Interdisciplinary Reviews: Computational Molecular Science* **2018**, *8*, e1327.
- [52] Steiner, T. Weak hydrogen bonding. Part 1. Neutron diffraction data of amino acid C α -H suggest lengthening of the covalent C-H bond in C-H \cdots O interactions. *J. Chem. Soc., Perkin Trans. 2* **1995**, 1315–1319.
- [53] Libowitzky, E. Correlation of O-H stretching frequencies and O-H \cdots O hydrogen bond lengths in minerals. *Monatshefte für Chemie / Chemical Monthly* **1999**, *130*, 1047–1059.
- [54] Steiner, T. The hydrogen bond in the solid state. *Angewandte Chemie International Edition* **2002**, *41*, 48–76.
- [55] Blazhnev, I. V.; Malomuzh, N. P.; Lishchuk, S. V. Temperature dependence of density, thermal expansion coefficient and shear viscosity of supercooled glycerol as a reflection of its structure. *The Journal of chemical physics* **2004**, *121*, 6435–6441.
- [56] Deng, H.; Callender, R. *Enzyme kinetics and mechanism Part E: Energetics of Enzyme Catalysis*; Methods in Enzymology; Academic Press, 1999; Vol. 308; pp 176 – 201.
- [57] Braga, D.; Grepioni, F.; Biradha, K.; Pedireddi, V. R.; Desiraju, G. R. Hydrogen Bonding in Organometallic Crystals. 2. C-H \cdots O Hydrogen Bonds in Bridged and Terminal First-Row Metal Carbonyls. *J. Am. Chem. Soc.* **1995**, *117*, 3156–3166.
- [58] Steiner, T. Lengthening of the Covalent X-H Bond in Heteronuclear Hydrogen Bonds Quantified from Organic and Organometallic Neutron Crystal Structures. *The Journal of Physical Chemistry A* **1998**, *102*, 7041–7052.
- [59] Sosa, G. L.; Peruchena, N. M.; Contreras, R. H.; Castro, E. A. Topological and NBO analysis of hydrogen bonding interactions involving C-H \cdots O bonds. *Journal of Molecular Structure: THEOCHEM* **2002**, *577*, 219 – 228.

- [60] The density data below T_g for glycerol taken from [61] are extrapolated from measurements of in crystalline state; i.e. the evolution below T_g is more accurately captured in sorbitol.
- [61] Naoki, M.; Ujita, K.; Kashima, S. Pressure-volume-temperature relations and configurational energy of liquid, crystal, and glasses of D-sorbitol. *The Journal of Physical Chemistry* **1993**, *97*, 12356–12362.
- [62] Sato, H.; Mori, K.; Murakami, R.; Ando, Y.; Takahashi, I.; Zhang, J.; Terauchi, H.; Hirose, F.; Senda, K.; Tashiro, K.; Noda, I.; Ozaki, Y. Crystal and Lamella Structure and C-H...OC Hydrogen Bonding of Poly(3-hydroxyalkanoate) Studied by X-ray Diffraction and Infrared Spectroscopy. *Macromolecules* **2006**, *39*, 1525–1531.
- [63] Particularly, our findings oppose earlier views that, based on their dielectric response, glycerol and sorbitol might represent two different types of glass formers (type A and type B glasses, respectively). Lunkenheimer, P.; Loidl, A. Dielectric spectroscopy of glass-forming materials: α -relaxation and excess wing. *Chem. Phys.* **2002**, *284*, 205 – 219, Strange Kinetics. Geirhos, K.; Lunkenheimer, P.; Loidl, A. Johari-Goldstein Relaxation Far Below T_g : Experimental Evidence for the Gardner Transition in Structural Glasses? *Phys. Rev. Lett.* **2018**, *120*, 085705. Kudlik, A.; Benkhof, S.; Blochowicz, T.; Tschirwitz, C.; Rössler, E. The Dielectric Response of Simple Organic Glass Formers. *J. Mol. Struct.* **1999**, *479*, 201–218. Lunkenheimer, P.; Loidl, A. In *The Scaling of Relaxation Processes*; Kremer, F., Loidl, A., Eds.; Springer International Publishing, 2018; pp 23–59.
- [64] Döfl, A.; Paluch, M.; Sillescu, H.; Hinze, G. From Strong to Fragile Glass Formers: Secondary Relaxation in Polyalcohols. *Phys. Rev. Lett.* **2002**, *88*, 095701.
- [65] Hensel-Bielowka, S.; Pawlus, S.; Roland, C. M.; Ziolo, J.; Paluch, M. Effect of large hydrostatic pressure on the dielectric loss spectrum of type-A glass formers. *Phys. Rev. E* **2004**, *69*, 050501.
- [66] Pronin, A.; Kondrin, M.; Lyapin, A.; Brazhkin, V.; Volkov, A.; Lunkenheimer, P.; Loidl, A. Glassy dynamics under superhigh pressure. *Phys. Rev. E* **2010**, *81*, 041503.
- [67] Gromnitskaya, E. L.; Danilov, I. V.; Lyapin, A. G.; Brazhkin, V. V. Elastic properties of liquid and glassy propane-based alcohols under high pressure: the increasing role of hydrogen bonds in a homologous family. *Phys. Chem. Chem. Phys.* **2019**, *21*, 2665–2672.
- [68] Floudas, G.; Paluch, M.; Grzybowski, A.; Ngai, K. *Molecular dynamics of glass-forming systems: effects of pressure*; Springer Science & Business Media, 2010; Vol. 1.
- [69] Grzybowski, A.; Paluch, M. In *The Scaling of Relaxation Processes*; Kremer, F., Loidl, A., Eds.; Springer, 2018; pp 77–119.
- [70] Ingebrigtsen, T. S.; Schröder, T. B.; Dyre, J. C. Isomorphs in Model Molecular Liquids. *The Journal of Physical Chemistry B* **2012**, *116*, 1018–1034.
- [71] Paluch, M.; Masiewicz, E.; Grzybowski, A.; Pawlus, S.; Pionteck, J.; Wojnarowska, Z. General rules prospected for the liquid fragility in various material groups and different thermodynamic conditions. *The Journal of Chemical Physics* **2014**, *141*, 134507.
- [72] Pawlus, S.; Paluch, M.; Grzybowski, A. Communication: Thermodynamic scaling of the Debye process in primary alcohols. *The Journal of Chemical Physics* **2011**, *134*, 041103.
- [73] Pedersen, U. R.; Bailey, N. P.; Schröder, T. B.; Dyre, J. C. Strong Pressure-Energy Correlations in van der Waals Liquids. *Phys. Rev. Lett.* **2008**, *100*, 015701.
- [74] Niss, K.; Hecksher, T. Perspective: Searching for simplicity rather than universality in glass-forming liquids. *J. Chem. Phys.* **2018**, *149*, 230901.
- [75] Meier, R.; Kruk, D.; Gmeiner, J.; Rössler, E. A. Intermolecular relaxation in glycerol as revealed by field cycling 1H NMR relaxometry dilution experiments. *J. Chem. Phys.* **2012**, *136*, 034508.
- [76] Flämig, M.; Hofmann, M.; Fatkullin, N.; Rössler, E. NMR RELAXOMETRY: THE CANONICAL CASE GLYCEROL. *J. Phys. Chem. B* **2019**, *?*, ?
- [77] Paluch, M.; Roland, C. The Avramov model of structural relaxation. *Journal of Non-Crystalline Solids* **2003**, *316*, 413 – 417.